3 Thermo- and Fluiddynamic Principles of Heat Transfer During Cooling

F. MAYINGER

3.1 Phenomena of Heat Transfer During Immersion Cooling

Heat transfer during immersion cooling is mostly connected with boiling because the temperature of the material to be cooled is usually higher than the boiling temperature of the liquid coolant. With boiling many kinds of complicated fluiddynamic and thermodynamic phenomena are interacting with each other. In spite of early starting research and many experimental and theoretical investigations boiling phenomena cannot be described on a fully theoretical basis until today. First systematic experiments originate from the 30th and here especially the investigations by Jakob [1], Fritz [2], Linke [3], Bosnjakovic [4] and Nukiyama [5] have to be mentioned. Already in these experiments it was observed that vapour bubbles are formed at very distinctive sites at the heated surface increasing in number with higher heat flux. Each bubble grows from a so-called nucleus which is assumed to be present in a small groove or local roughness on the heated surface. The heat is not directly transferred from the surface to the vapour bubble, but it first enters the liquid, being adjacent to the surface, superheats a thin liquid layer and by this creates a thermodynamic metastable situation for a very short period. If the nucleus is big enough or the superheating of the thin liquid layer is high enough, a bubble is formed which gets its heat and mass—vapour—from this superheated liquid layer, called boundary layer.

The vapour in the bubble must be of higher pressure p_v than the surrounding liquid because in addition to the liquid pressure p_l the surface tension σ acts on the phase interface between bubble and liquid as can be shown with a simple force balance. Equation (1) gives this force balance for a spherical bubble being in equilibrium i.e. not growing and not shrinking.

$$p_v - p_l = \frac{2\sigma}{R}. \tag{3.1}$$

If we use the Clausius Clapeyron equation in addition

$$\frac{dp}{dT} = \frac{\Delta h_v}{(v_v - v_l)T} \tag{3.2}$$

well-known from thermodynamics we can derive an expression describing the

relationship between the radius of the bubble and the necessary superheating of the vapour in it. By this we get some information about the metastable situation of the liquid in the boundary layer. If we bring Eq. (3.1) and Eq. (3.2) together and integrate with the simple assumption that the vapour can be treated as ideal gas and that the specific volume of the liquid is negligibly small compared with that of the vapour, we can easily get a rough estimation of the superheating temperature $(T_v - T_s)$ being necessary to allow a bubble of the radius R to grow.

$$R = \frac{2\sigma}{\Delta h_v \cdot \rho_v} \cdot \frac{T_s}{T_v - T_s} \tag{3.3}$$

Equation (3.3) shows that with increasing superheating of the liquid beyond the saturation temperature T_s smaller nuclei at the heated surface can become active. On the other side however, the superheating of the surface is a function of the heat flux being transferred through the solid material to it. Usually the surface of a solid material contains roughness sites of different size and, therefore, the number of the activated nuclei—i.e. of the locations, where bubbles are formed at the surface—is increasing with higher heat flux. This increasing of the number of activated nuclei results in a more intensive fluiddynamic mixing of the liquid at the heated surface. Both together, namely the mass transport in the bubble in form of vapour and the microscopic turbulence with its drift flux behind the bubble improve the heat transfer conditions. Therefore, one can expect that the heat transfer coefficient is improved with increasing heat flux during boiling.

A simple experiment which was demonstrated in the literature by Nukiyama [5] proves this deliberation. Nukiyama measured at and above a heated plate the surface temperature T_W and the liquid temperature T_F and correlated both with the heat flux $\dot{q}$. In Fig. 3.1 the heat flux and the heat transfer coefficient α are plotted versus the temperature difference between the heated surface and the boiling liquid in a logarithmic scale as Nukiyama did it. At low heat flux the energy transport is managed at the wall by liquid free convection only, and evaporation occurs only after the superheated liquid reaches the upper surface of the pool where the radius of the phase interface is almost infinite.

The onset of bubble formation at the heated wall, i.e. the bubble boiling causes a sudden change in the slope of the curves, shown in Fig. 3.1, because the heat transfer conditions are now instantaneously improved. Increasing the heat flux more and more, one finally reaches a situation, where the transport phenomenon with bubble boiling becomes hydrodynamically unstable, because due to the dense bubble population and the huge vapour flow, the liquid will be prevented from flowing down to the heated solid surface, and this impairment of liquid flow to the wall changes the boiling situation. Suddenly a thin but coherent vapour film is formed at the heating surface separating the liquid from it and now bubble boiling changes into the so-called film boiling. This sudden change is called "Departure from Nucleate Boiling" (DNB) and the heat flux at which it occurs is referred to as the "Critical Heat Flux" (CHF). The heat transfer coefficient reaches its maximum shortly before DNB is observed.

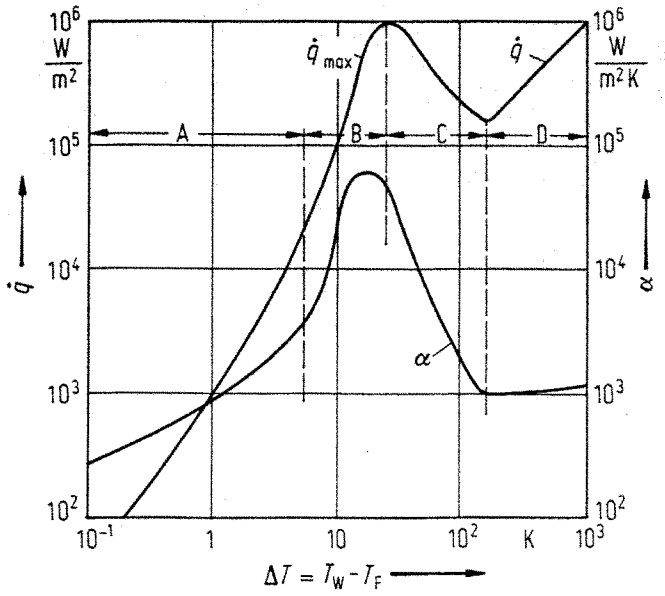

Fig. 3.1. Nukiyama curve for boiling, *A* free convection, *B* nucleate boiling, *C* transition boiling, *D* film boiling

If we increase the heat flux at the DNB-point only a little more we can observe a sudden and large jump in the wall temperature which may result—e.g. with water of ambient pressure—in several 100 K. At higher pressures this temperature-jump is not so large and at very high pressures—near the critical point—the temperature may even continuously change with heat flux after the DNB, but still to a large extent.

After this unstable situation at and immediately above the DNB-point, the temperature of the wall is again continuously rising with increasing heat flux, however, the q-ΔT-curve is now much flatter as it was before departure from nucleate boiling. As seen from Fig. 3.1, the heat transfer coefficient drops down when DNB is exceeded by one or two orders of magnitude.

If we now lower the heat flux, we do not observe the sudden jump at that point, where we arrived at after exceeding the DNB-point when heating, but the temperature is still continuously decreasing until the q-ΔT-curve reaches its minimum. Here the temperature instantaneously falls and the situation returns to the nucleate boiling branch of the curve. With further reduction of the heat flux the temperature is then continuously, but only slightly decreasing along the nucleate boiling line.

Situations in the region *C* on this curve—in the literature called Nukiyama-curve—can only be reached if we change the heating conditions. Instead of imposing a given heat flux, we can imagine that we keep the wall at a given constant temperature by appropriate means, for example by heating with liquid metal. Then we can adjust a temperature in the region *C*, and we shall observe a fluctuating behaviour of the boiling conditions between nucleate and film boiling and with intermediate wetting of the wall.

For situations in the region *D* only film boiling can be observed and the wall remains unwetted by the liquid. The temperature at the minimum is called

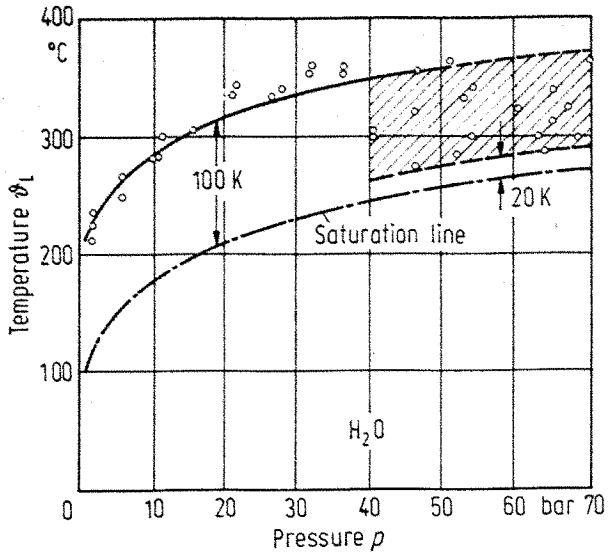

Fig. 3.2. Rewetting temperature (Leidenfrost-temperature) for water according to Hein [7]

Leidenfrost-temperature or rewetting-temperature, because by lowering the heat flux below that value, the wall becomes rewetted again. The temperature at which this rewetting occurs is still under discussion and research in the literature. Sometimes theories predicting the so-called homogeneous nucleus-formation-temperature are used, however, they give much too high rewetting temperatures. Yao [6] confirmed earlier observations that the rewetting temperature is strongly depending on the surface conditions, such as roughness or thin coating layers and also on the thermal conductivity of the material at which rewetting occurs. Yao found that on thermally stable substances—solid materials—rewetting starts much earlier than the homogeneous nucleus-formation-theory predicts. The rewetting- or Leidenfrost-temperature, is also a slight function of the pre-cooling history.

A detailed survey on the rewetting by flooding and on the Leidenfrost-temperature is given by Hein [7]. According to his investigations and measurements the rewetting temperature of water is at low pressure—between 1 and 40 bar—approximately 100 K above the saturation temperature as Fig. 3.2 shows. This means that the vapour layer at the wall breaks down if film boiling or thermal conduction to a near-by rewetted area could cool down the surface of the material to a temperature less than 100 K above the saturation temperature. At higher pressures the difference between saturation temperature and rewetting temperature becomes smaller and it can be reduced down to 20 K. The measurements, however, show a wide range of scattering. This is not so much due to the uncertainty of the experimental readings, but the rewetting temperature is strongly influenced by the surface conditions, roughness and coating layers, e.g. by oxide formation.

With other substances the situation is similar. In Fig. 3.3 rewetting temperatures of the refrigerant R12 are plotted versus the pressure. Similar to water also in this substance the difference between rewetting temperature and

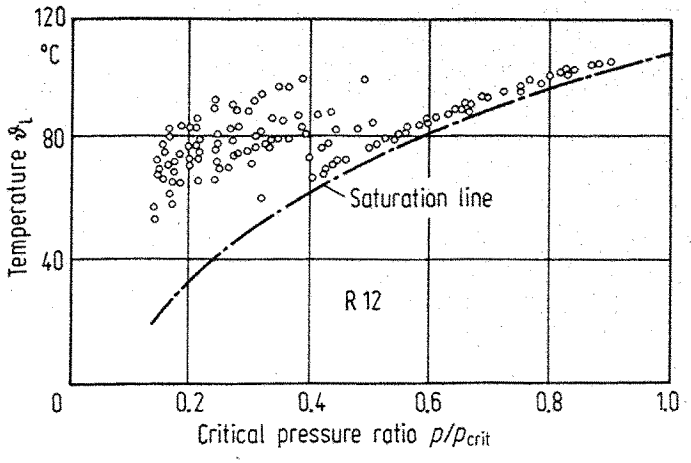

Fig. 3.3. Rewetting temperature (Leidenfrost-temperature) for the refrigerant R12 according to Hein [7]

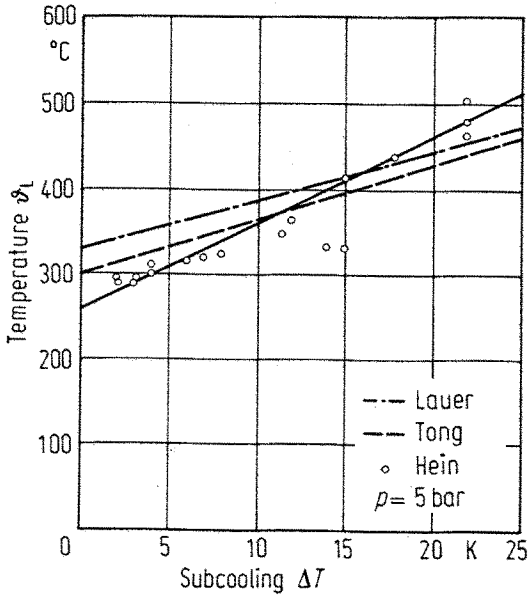

Fig. 3.4. Influence of the subcooling of the liquid onto the rewetting (Leidenfrost-temperature) in water

saturation temperature decreases with increasing pressure. At high pressures this substance even shows a much more homogeneous behaviour than water.

As mentioned before, the heat transfer conditions are influencing the rewetting temperature also. Improved cooling conditions exist when the liquid is subcooled because the condensation of the vapour at the phase interface between vapour layer and liquid produces strong turbulence and acceleration of the liquid mass towards the hot surface. By this, liquid is impinged to the wall and rewetting can start earlier—at higher surface temperatures—compared with film boiling in saturated liquids. This observation was confirmed by Lauer [8], Tung [9] and Hein [7]. As demonstrated in Fig. 3.4 the rewetting-temperature is increasing linearly with the subcooling of the liquid and for example water, 25 K below the saturation temperature and at 5 bar, can wet a hot wall already at 500 °C.

The thermo- and fluiddynamic situation with nucleate boiling is even more complicated than with film boiling. In the literature many theoretical and

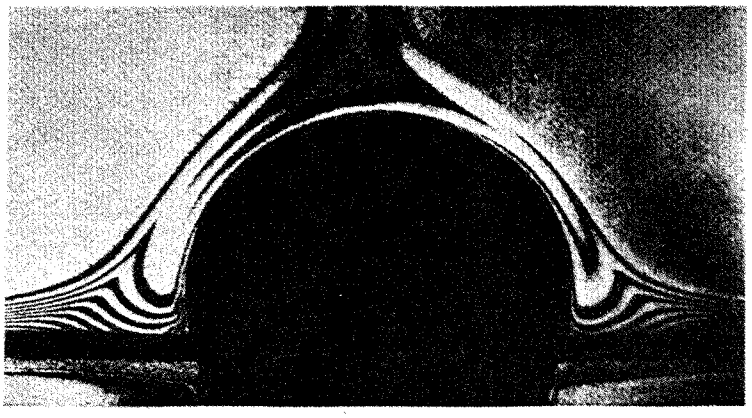

Fig. 3.5. Temperature field around a bubble growing on a wire in water ($p = 0.3$ bar, $q = 30\,\mathrm{W/cm^2}$, subcooling 2 K)

experimental investigations on bubble formation and bubble growth can be found. One should mention e.g. the papers by Forster and Zuber [10], Hahn and Griffith [11], Plesset and Zwick [12], Beer [13] or Winter [14]. The occurrences with bubble growth are controlled by various parameters and forces. In the very first moment after the necessary superheating of the liquid directly at the wall is reached, the growth of the bubble out of the nucleus is governed by the inertia of the liquid which has to be pushed away by the growing bubble. This first evaporation step causes a temperature drop in the liquid near the phase interface and the pressure in the bubble is lowered equivalently to the cooling of the liquid. For further evaporation, liquid has to be transported to the phase interface from surrounding areas and, therefore, during this second period of bubble growth heat- and masstransport in the liquid is governing the bubble growth. To understand these heat- and masstransport phenomena better, it may be helpful to get information on the temperature conditions near the wall and at the phase interface of the bubble.

Optical measuring techniques are good tools to record the very quickly changing temperature situation near a growing bubble. A convenient method to be handled is the holographic interferometry [15]. An example of a holographic interferogram taken of the temperature field around a bubble which is growing on a heated wire is shown in Fig. 3.5. The light and dark fringes in this interferogram represent—in a first approximation—isotherms in the liquid. The temperature field around the bubble is influenced by a proceeding bubble which left the heated wire a few milliseconds before and which is only "visible" in this picture by its drift flow. The superheated boundary layer around the wire can be clearly seen on the left side of Fig. 3.5. The temperature field around a bubble growing on a heated flat surface and its life-history is shown in Fig. 3.6. When the nucleus becomes active, the bubble starts growing into the superheated boundary layer due to evaporation out of this layer. After 4 ms the bubble starts to shrink and the bubble is disappeared after 7 ms. The reason for this is that the water flowing over the heated surface is subcooled

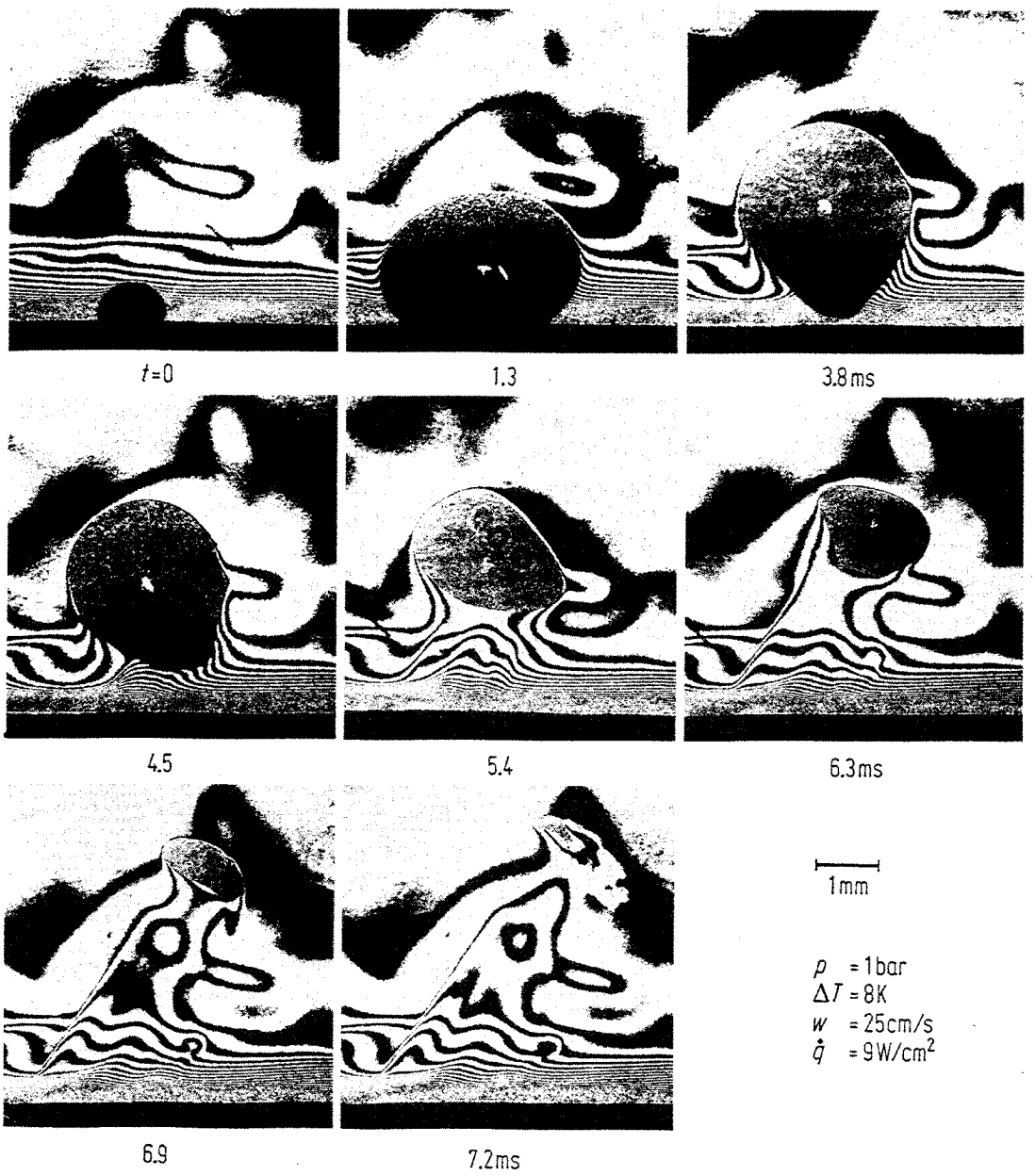

Fig. 3.6. Boundary layer and bubble formation with boiling in water at 1 bar, water-temperature 8 K below saturation temperature, velocity $w = 0.25\,\text{m/s}$, heat flux $q = 9\,\text{W/cm}^2$

—8 K below saturation temperature—and only an approximately 1 mm thick boundary layer is superheated due to heat addition. In this boundary layer a large temperature gradient exists as the densely situated fringes—representing isotherms—show. Evaluating this interference fringes, one finds that the liquid adjacent to the wall is approximately 10 K superheated above the saturation temperature. The total temperature difference between the wall and the bulk therefore is 18 K.

3.2 Single Phase Convection

Without convection—enforced by natural buoyancy or by pressure differences—heat is transported by molecular conduction only. With convecting fluids—liquid or gas—the heat transport is strongly supported or almost exclusively managed by the movement of the fluid. This heat transport by the movement of the fluid can easily be considered in a laminar fluid flow. To do this, we look at a rectangular element having edge distances dx, dy, and dz, as shown in Fig. 3.7. In z-direction, i.e. vertically to the drawing plain, the temperature is assumed to be constant. Then the heat fluxes $d\dot{Q}_{\lambda,x,\text{in}}$, $d\dot{Q}_{\lambda,y,\text{in}}$, enter the volume element and the heat fluxes $d\dot{Q}_{\lambda,x,\text{out}}$ and $d\dot{Q}_{\lambda,y,\text{out}}$ leave this element. If this volumetric element in addition is penetrated by a fluid flow in x-direction having the velocity w then the entering mass flow-rate

$$d\dot{M} = \varrho w dA = \varrho w dy dz \tag{3.4}$$

brings with it the specific enthalpy h and the enthalpy flux due to this flow—or convenction—can be expressed by the equation

$$d\dot{Q}_{\text{conv,in}} = \varrho w h dA = \varrho w h dy dz \tag{3.5}$$

In steady state flow the enthalpy flux leaving the volumetric element is increased by the temperature rise $d\vartheta$ if heat is added to the volumetric element by conduction. In a detailed consideration we would also have to take into account the kinetic energy and the dissipated energy in this element due to the flow. Here we assume that the contributions of these kinds of energy are small compared with the enthalpy flow. In addition we shall assume steady state conditions which means that the flow velocity and also the heat fluxes due to heat conduction are temporarily not changed in the volumetric element.

The energy balance can then be written in a simple way for this element:

$$(d\dot{Q}_{\lambda,x,\text{in}} - d\dot{Q}_{\lambda,x,\text{out}}) + (d\dot{Q}_{\lambda,y,\text{in}} - d\dot{Q}_{\lambda,y,\text{out}}) + (d\dot{Q}_{\text{conv,in}} - d\dot{Q}_{\text{conv,out}}) = 0. \tag{3.6}$$

With the expressions for the molecular heat conduction and the convective

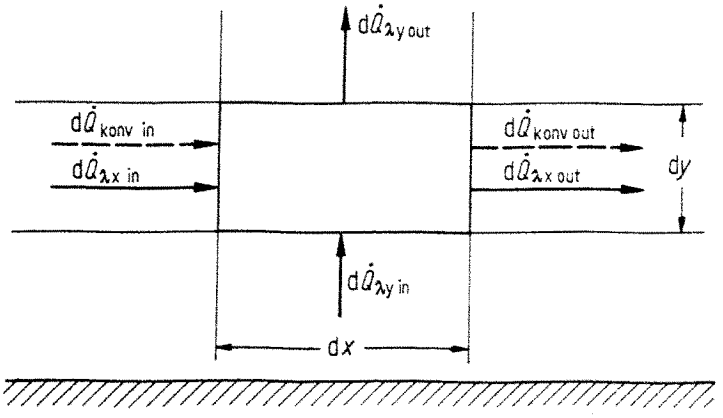

Fig. 3.7. Heat balance with molecular (conductive) and convective transport

enthalpy transport, the energy balance then has the form

$$\frac{\partial}{\partial x}\left(-\lambda dA\frac{\partial \vartheta}{\partial x}\right)+\frac{\partial}{\partial y}\left(-\lambda dA\frac{\partial \vartheta}{\partial y}\right)+\frac{\partial}{\partial x}(\varrho w h dA)=0 \tag{3.7}$$

By rearranging this equation and by substituting

$$h=cd\vartheta \tag{3.8}$$

and with the thermal diffusivity $a=\lambda/\varrho\cdot c$ we get the well-known energy-transport equation in two-dimensional form.

$$a\left(\frac{\partial^2 \vartheta}{\partial x^2}+\frac{\partial^2 \vartheta}{\partial y^2}\right)=w\frac{\partial \vartheta}{\partial x}. \tag{3.9}$$

With most practical applications and for almost all fluids—with exception of liquid metals—the molecular heat transport, i.e. the heat conduction in x-direction, is small compared with the energy transport by convection, and we therefore can neglect the longitudinal heat conduction. Doing this, Eq. (3.9) reads:

$$a\frac{\partial^2 \vartheta}{\partial y^2}=w\frac{\partial \vartheta}{\partial x}. \tag{3.9a}$$

For solving Eqs. (3.9) and (3.9a) we need information on the flow velocity in all 3 directions x, y, and z which we get from the laws of fluiddynamics. A very general fluiddynamic law e.g. is formulated in the Navier–Stokes-equation which is a balance equation for the forces acting on a fluid element

$$\begin{aligned}
w_x\frac{\partial w_x}{\partial x}+w_y\frac{\partial w_x}{\partial y}+w_z\frac{\partial w_x}{\partial z}&=-\frac{1}{\varrho}\frac{\partial p}{\partial x}+\nu\left(\frac{\partial^2 w_x}{\partial x^2}+\frac{\partial^2 w_x}{\partial y^2}+\frac{\partial^2 w_x}{\partial z^2}\right)\\
w_x\frac{\partial w_y}{\partial x}+w_y\frac{\partial w_y}{\partial y}+w_z\frac{\partial w_y}{\partial z}&=-\frac{1}{\varrho}\frac{\partial p}{\partial y}+g+\nu\left(\frac{\partial^2 w_y}{\partial x^2}+\frac{\partial^2 w_y}{\partial y^2}+\frac{\partial^2 w_y}{\partial z^2}\right)\\
w_x\frac{\partial w_z}{\partial x}+w_y\frac{\partial w_z}{\partial y}+w_z\frac{\partial w_z}{\partial z}&=-\frac{1}{\varrho}\frac{\partial p}{\partial z}+\nu\left(\frac{\partial^2 w_z}{\partial x^2}+\frac{\partial^2 w_z}{\partial y^2}+\frac{\partial^2 w_z}{\partial z^2}\right).
\end{aligned} \tag{3.10}$$

From the Navier–Stokes-equation dimensionless numbers as the Reynolds-number

$$Re=\frac{wL}{\nu}\quad\text{or}\quad Re=\frac{wD}{\nu} \tag{3.11}$$

or the Grasshof-number

$$Gr=\frac{L^2 g\beta\Delta\vartheta}{w\nu}\,Re=\frac{L^3 g\beta\Delta\vartheta}{\nu^2} \tag{3.12}$$

were derived by writing this equation in a dimensionless form [16]. Doing the

same with the energy equation (Eq. (9)) we get the Peclet-number.

$$Pe = \frac{wL}{a}. \tag{3.13}$$

Finally the quotient of the Peclet- and Reynolds-number forms the Prandtl-number.

$$Pr = \frac{Pe}{Re} = \frac{v \cdot \varrho \cdot c}{\lambda} = \frac{v}{a}. \tag{3.14}$$

If we now consider the situation directly at the wall where an infinitely thin stagnant liquid layer exists and introduce the well-known definition for the heat transfer coefficient α

$$\alpha = \frac{\dot{Q}}{A(T_{\text{Wall}} - T_{\text{Bulk}})} = \frac{\dot{Q}}{A(\vartheta_{\text{Wall}} - \vartheta_{\text{Bulk}})} \tag{3.15}$$

we can write a simple energy balance at this position just by taking into account that the heat conducted through this infinite thin stagnant liquid layer must be equal to the total heat transport from the wall to the fluid.

$$\lambda A \frac{\partial T}{\partial y} = \alpha A(T_{\text{Wall}} - T_{\text{Bulk}}). \tag{3.16}$$

In the Eqs. (3.15) and (3.16) T_{Bulk} represents the temperature of the fluid in a position far away from the wall. By rearranging and writing Eq. (3.16) in a dimensionless form we finally can derive the Nusselt-number.

$$Nu = \frac{\partial(T/\Delta T)}{\partial(y/L)} = \frac{\alpha L}{\lambda} = \frac{\alpha D}{\lambda}. \tag{3.17}$$

We shall now consider a very simple example of a heat transfer problem, namely the heat transport to a flat plate from a fluid flowing longitudinally over it, and the solutions of the energy- and Navier–Stokes-equation will be demonstrated in a simple and dimensionless form for these fluiddynamic conditions. We assume that the flat plate as shown in Fig. 8 is positioned in a fluid flow of the

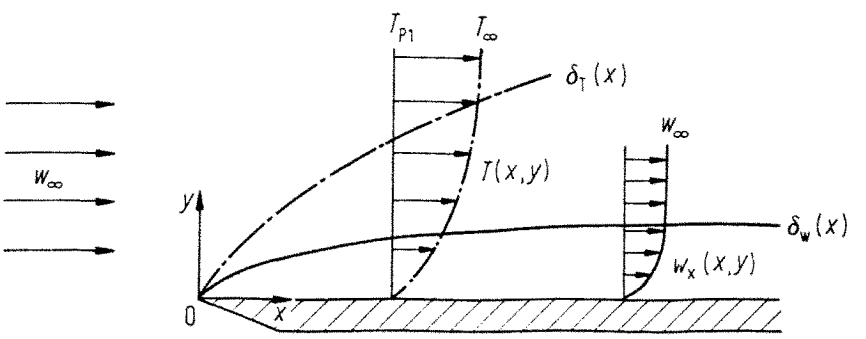

Fig. 3.8. Boundary layers of velocity and temperature on a plate with longitudinal flow

velocity w_∞. In the immediate vicinity of the plate surface this velocity w_∞ is decelerated by the friction at the wall. Only in a distance away far enough from the wall the upstream-velocity w_∞ remains uninfluenced. Between the wall and the uninfluenced environment a velocity profile is formed as sketched in Fig. 3.8. In a similar way the temperature of the fluid above the plate behaves. In a distance far enough away from the plate the temperature of the fluid is not influenced by the heat addition to the plate and is equal to the upstream-temperature. Near the plate surface the fluid temperature approaches the plate temperature.

Starting from the front edge of the plate, a laminar flow zone will be formed, even if the upstream-flow-conditions are turbulent. This laminar zone is increasing in its thickness over the plate length, starting from the front plate edge. This continues until turbulence starts.

It is usual in the literature to define a boundary-layer thickness δ_w as that distance from the plate surface, where the velocity just reaches 99% of the upstream-velocity. In a similar way also a temperature-boundary-layer thickness δ_T is defined as that distance from the plate surface, where the fluid-temperature is 99% of the temperature in the upstream undisturbed region. So we see that the heat transport is mainly restricted to the region where the boundary-layer exists.

If we want to have some information about the boundary-layer thickness we have to solve the Navier–Stokes-equation and the energy equation. In addition we need the continuity equation. In its simplest form we can write the Navier–Stokes-equation by assuming that the pressure gradient vertically to the plate can be neglected and that there is also no friction due to any flow in this perpendicular direction.

$$w_x \frac{\partial w_x}{\partial x} + w_y \frac{\partial w_y}{\partial y} = -\frac{1}{\varrho}\frac{\partial p(x)}{\partial x} + \nu \frac{\partial^2 w_x}{\partial y^2} \tag{3.18}$$

Equation (3.18) is called boundary-layer equation and was formulated by Prandtl in 1904. A first solution for this equation was given by Blasius, who made the additional simplifying assumption that the pressure gradient dp/dx longitudinally to the plate can be neglected also. For the above mentioned boundary layer thickness Blasius found the equation

$$\frac{\delta(x)}{x} \approx \frac{5}{\sqrt{Re}} \quad \text{or} \quad \frac{\delta(x)}{L} \approx \frac{5}{\sqrt{Re_L}}\sqrt{\frac{x}{L}}. \tag{3.19}$$

From this equation for the boundary-layer thickness Blasius finally derived an expression for the friction factor ψ in laminar flow.

$$\psi(x) = \frac{0.664}{\sqrt{Re_x}} \tag{3.20}$$

As well-known, this friction factor is defined in laminar flow as

$$\psi(x) = 2\frac{\tau_{\text{Wall}}(x)}{\varrho w_{\text{Bulk}}^2} \approx 2\frac{\tau_{\text{Wall}}(x)}{\varrho w_\delta^2}. \tag{3.21}$$

For calculating the heat transfer conditions we have to take into account the energy equation in addition, and for simplicity we assume that there is heat conduction only perpendicular to the plate surface.

$$w_x\frac{\partial \vartheta}{\partial x} + w_y\frac{\partial \vartheta}{\partial y} = a\frac{\partial^2 \vartheta}{\partial y^2}. \tag{3.22}$$

For $Pr = 1$ and constant wall temperature the exact solution for the heat transfer using the equations by Blasius and the energy equation is:

$$Nu_x = 0.332\sqrt{Re_x}. \tag{3.23}$$

For fluids, where the Prandtl-number is not equal to 1, only approximate solutions exist as for example:

$$Nu_x = \frac{\alpha x}{\lambda} = 0.332\, Re_x^{1/2} \cdot Pr^{1/3}. \tag{3.23a}$$

By comparing Eqs. (3.20) and (3.23), we very easily can see the connection between momentum—and heat transport

$$\frac{Nu}{Re\,Pr} = \frac{\psi}{2}; \tag{3.24}$$

which is called the "Reynolds-analogy".

For turbulent boundary conditions the circumstances are much more complicated. In the literature there are several models showing possibilities for taking into account the turbulent cross flow fluctuations or the eddy diffusivity. For practical use, however mostly empirical correlations are proposed which are similar to Eqs. (3.23) or (3.23a).

$$Nu = CRe^m\, Pr^n. \tag{3.25}$$

The exponent n of the Prandtl-number is a little different for a heated wall ($n = 1/3$) and for a cooled wall ($n = 0.4$). The flow velocity and by this the Reynolds-number, however, is of stronger influence in turbulent flow and the exponent m, therefore, has values of 0.7–0.8. The Reynolds-analogy in its simplest form is similar to that in laminar flow (Eq. (3.24)), however, the quotient between heat transfer and friction is smaller.

$$\frac{Nu}{Re\,Pr} = \frac{\psi}{8}. \tag{3.26}$$

If we apply this turbulent Reynolds-analogy (Eq. (3.26)) to the well-known

friction law by Blasius

$$\psi = \frac{0.3164}{Re^{0.25}} \tag{3.27}$$

we get for fluids with $Pr = 1$

$$Nu = 0.0396 \cdot Re^{0.75} = CRe^{m} \tag{3.28}$$

which corresponds in its form with Eq. (3.25) and which is the basis for many correlations predicting heat transfer in heat exchanging components.

3.2.1 Heat Transfer Equations for Forced Convection

Heat transfer and fluid flow, however, are also depending on the geometrical form of the heated or cooled surface. Therefore, in the literature we find different—mostly empirical—correlations for predicting heat transfer in different configurations. For laminar flow in tubes and channels (up to $Re = 2300$) Schlünder [17] recommends the simple correlation

$$Nu = \frac{\alpha D_i}{\lambda} = \sqrt[3]{3.66^3 + 1.62^3 \, Re \, Pr \frac{D_i}{L}}, \tag{3.29}$$

which is also valid in the entrance region of the channel.

Applying this or other heat transfer-equations, it is important to use the correct temperature—the so-called reference temperature—for selecting the values for the thermodynamic properties in the dimensionless numbers. There is a temperature gradient perpendicular and longitudinal to the heat exchanging wall, and usually the reference temperature—sometimes also called mean bulk-temperature—is calculated as the arithmetic mean value between the entrance and the outlet temperature in the channel or tube.

$$T_{Bulk} = (T_{in} - T_{out})/2. \tag{3.30}$$

Sometimes also the logarithmic mean value is used.

For turbulent flow in tubes or channels Colburn derived from the Reynolds-analogy the simple correlation

$$Nu = \frac{\alpha D_i}{\lambda} = 0.023 \, Re^{0.8} \cdot Pr^{1/3}, \tag{3.31}$$

which gives good results for not too high heat fluxes and in the range $10^4 < Re < 10^5$ and $0.5 < Pr < 100$. It is not applicable in the entrance region, because there the heat transfer coefficiences are higher than Eq. (3.31) predicts. Hausen [18] presented a correlation for a very large range of Reynolds-numbers,

namely from laminar flow up to the highly turbulent conditions of $Re = 2.5 \cdot 10^5$, which is also valid in the entrance region.

$$Nu = 0.0235(Re^{0.8} - 230)(1.8\,Pr^{0.3} - 0.8)\cdot\left[1 + \left(\frac{D_i}{L}\right)^{2/3}\right]\left(\frac{\eta_{Bulk}}{\eta_{Wall}}\right)^{0.14}. \tag{3.32}$$

3.2.2 Heat Transfer Equations for Natural Convection

Free convection is driven by buoyancy forces and not by pressure drop. Therefore the heat transfer correlations for convection are formed with the Grashof-number (Eq. 3.12) instead of the Reynolds-number. The heat transfer coefficient is again expressed by the Nusselt-number and the correlations for calculating the heat transfer in free convection have the form

$$Nu = f(Gr, Pr). \tag{3.33}$$

In closed cavities free convection only starts if:

$$Gr\,Pr > 1700. \tag{3.34}$$

The Grashof-number for closed cavities is formed with the distance between the two vertical walls.

For quenching free convection around bodies in a pool is of more interest. For a vertical plate Rohsenow an Choi [20] derived a correlation, using the balance equations, which is valid for laminar flow along the plate

$$\frac{Nu_x}{(Gr_x/4)^{1/4}} = \frac{0.676\,Pr^{1/2}}{(0.861 + Pr)^{1/4}}. \tag{3.35}$$

In (3.35) the Nusselt- and the Grashof-number are functions of the flow path, i.e. of the distance from the lower edge of the plate. In the Grashof-number the difference of the temperatures at the plate surface and in the fluid where it is not yet affected by heat transfer has to be inserted as characteristic temperature difference. If the plate is cooled, the flow goes downward and therefore, the flow path has to be counted from the upper edge of the plate.

One can also rearrange Eq. (3.35) to derive a mean Nusselt-number and Eq. (3.35) then reads

$$\frac{Nu_m}{(Gr/4)^{1/4}} = \frac{0.902\,Pr^{1/2}}{(0.861 + Pr)^{1/4}}. \tag{3.36}$$

Laminar boundary layers are observed at vertical flat plates up to $Gr\,Pr = 10^8$ Closed solutions for turbulent boundary layers are more complicated. For Prandtl-numbers between 1 and 10 one can, however, use the simple correlation

$$Nu_m = 0.13(Gr \cdot Pr)^{1/3} \tag{3.37}$$

with good accuracy.

3.3 Two Phase Heat Transfer

Discussing heat transfer with single-phase forced convection, we realized that the heat transfer coefficient is not a function of the temperature difference between the wall and the fluid. With free convection we found that density differences, caused by temperature differences, are impelling the heat transport and, therefore, the heat transfer coefficient is here depending on the temperature difference between wall and fluid. Boiling and heat transfer in two-phase flow are always connected with phase change which results in very large volume changes due to the density differences between liquid and vapour. Therefore, one can expect a priori that heat transfer is strongly influenced by buoyancy forces, however, also by dynamic forces originating from the bubble growth. These forces are affecting the boundary layer to such an extent that heat transfer with boiling allows high heat fluxes and cannot be improved very much by superimposing forced convection. Therefore, one reaches almost the same values in free and in forced convection. As we have seen when discussing the boiling phenomena, the number of activated nuclei per unit of area increases with rising wall temperature and by this with higher heat flux. Therefore one can expect that the heat transfer coefficient is a function of the heat flux because of the agitating effect of the growing, departing and rising bubbles. From these simple deliberations one can derive the correlation

$$\alpha = Cq^{n}, \tag{3.38}$$

where, however, the constant C differs from fluid to fluid and is a function of the pressure and the surface roughness. For more general validity, therefore, one would have to extend Eq. (3.38) to the form

$$\alpha = C_{F} \cdot C_{w} \cdot F(p) q^{n} \tag{3.39}$$

where C_{F} represents the properties of the liquid, C_{w} the roughness and the thermal conductivity of the wall, and the influence of the pressure is expressed by $F(p)$.

3.3.1 Free Convection Boiling

Considering the formation and movement of the bubbles in the liquid, it is possible to develop physical models and empirical correlations for the heat transfer coefficient with pool boiling. However, as seen in Fig. 3.1, we always have to observe whether—depending on the heat flux and the surface temperature—the system is in nucleate or in film boiling conditions. Both conditions are separated by the so-called boiling crisis and for knowing the heat flux at which nucleate boiling changes into film boiling, we have to discuss critical heat flux correlations.

Correlations using dimensionless numbers for boiling heat transfer have a more general validity than Eqs. (3.38) and (3.39). Dimensionless numbers for

pool boiling are formed with the transport properties of the substance, the heat flux density and the thermodynamic state—i.e. the boiling temperature. Correlations formed with such dimensionless groups are of empirical character, too. However, they have the benefit that they are valid for several substances and for a wide range of pressure and saturation temperature. An additional influence onto the heat transfer with boiling comes from the roughness and the thermal conductivity of the solid surface on which boiling occurs. Most of the correlations in the literature, however, neglect these effects because up to now, they are not well enough understood. On very smooth surfaces, for example on glas, it may happen that nucleate boiling is suppressed and after a high superheating of the liquid suddenly film boiling occurs. Technical surfaces—e.g. of metal, —however, are usually rough enough that a large number of bubble nuclei can form, and there the influence of an additional roughness is small.

For calculating the heat transfer with nucleate boiling on metallic surfaces, here the equation by Stephan and Preusser [21] is presented

$$Nu = \frac{\alpha D_{\text{bub}}}{\lambda_\rho} = 0.1 \left[\frac{qD_{\text{bub}}}{\lambda_l \vartheta_s}\right]^{0.674} \left[\frac{\varrho_v}{\varrho_l}\right]^{0.156} \left[\frac{\Delta h_v D_{\text{bub}}}{a_l^2}\right]^{0.341} \cdot \left[\frac{a_l^2 \varrho_l}{\sigma D_{\text{bub}}}\right]^{0.350} \left[\frac{\eta c}{\lambda}\right]_l^{-0.162} \tag{3.40}$$

Equation (3.40) is written in the power and product form which is familiar from the correlations for single-phase convection. It contains dimensionless groups which are formed with thermodynamic properties, the saturation temperature and the heat flux density. In addition some groups in this correlation contain the diameter of the bubble, when separating from the surface. This bubble diameter can be calculated by considering the equilibrium of the separating force due to buoyancy and of the holding force due to surface tension.

$$D_{\text{bub}} = 0.0146\beta \left(\frac{2\sigma}{g(\varrho_l - \varrho_v)}\right)^{0.5}. \tag{3.41}$$

For the contact angle β between the bubble and the solid surface, one has to insert into Eq. (3.41) the following values:

For water 45°,
for cryogenic substances 1°,
for hydrocarbons including refrigerants 35°.

In Eq. (3.40) a_l is the thermal diffusivity of the liquid formed with its thermal conductivity, density and specific heat.

$$a_l = \frac{\lambda_l}{\varrho_l c_l}. \tag{3.42}$$

For water and if the claim with respect to accuracy of the predicted values is

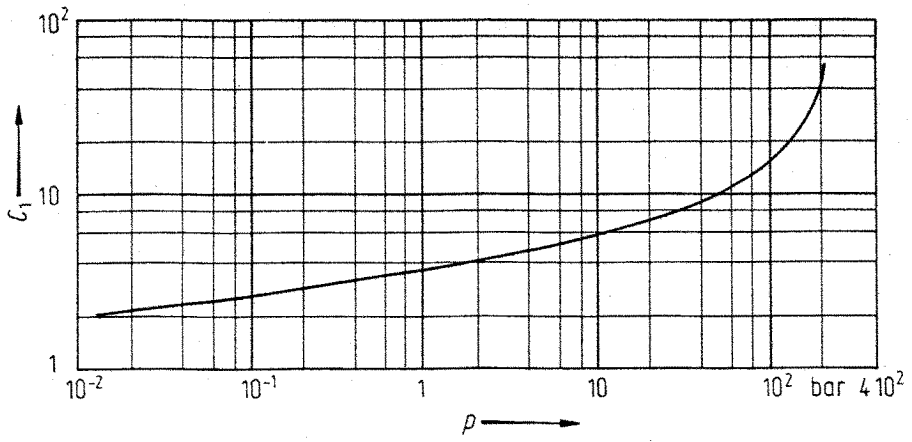

Fig. 3.9. Constant C_1 in Eq. (43) as a function of the pressure (water)

not too high, one can also use the much simpler equation

$$\alpha_{\text{boil.}} = C_1 \dot{q}^{0.673}, \tag{3.43}$$

where C_1 is a factor which depends on the pressure in the system and whose value can be taken from Fig. 3.9.

3.3.2 Forced Convection Boiling

With forced convection boiling the heat transfer situation changes as far as a velocity profile is superimposed onto the microconvection, produced by the departing bubbles near the wall. However, looking more in detail, one realizes that this velocity profile is only weakly influencing the very first phase of the bubble formation, the nucleation. Due to friction forces the velocity at the wall is zero and, in addition, growing and departing bubbles decelerate the velocity in the boundary layer near the wall.

For activating a nucleus only the superheating in the boundary layer in the immediate vicinity of the wall is of influence, also in forced convection flow. Different is the situation for the bubble growth and the bubble departure. If we consider the forces acting on a growing and departing bubble in forced convection, we have to take into account also the resistance and the momentum force due to the flow, in addition to the forces by buoyancy and surface tension. So the heat transfer with nucleate boiling is slightly improved by the forced convection compared with pool boiling. There are attempts in the literature to calculate the heat transfer in forced convection nucleate boiling by superimposing the effect of microconvection, produced by bubble departure and that of forced convection due to the superimposed directed flow. Rohsenow [22] presented a correlation in which the heat flux from the wall is the sum of two parts, one is formulated with the heat transfer coefficient for nucleate pool boiling and the other one with the heat transfer coefficient for single-phase forced convection. Compared with single-phase forced convection, the heat transfer coefficient for

nucleate pool boiling, however, is larger by one or two orders of magnitude. So the contribution of the forced convection for improving the heat transfer with boiling is small and can be neglected in most cases. Therefore, Eq. (3.40) is frequently used for forced convection boiling also.

A different situation is given, when dipping a body, i.e. a plate, into a liquid. As long as the surface temperature of the body is not too high—that is below the Leidenfrost-temperature—we can expect nucleate boiling. Here the free convection, due to buoyancy forces, is superimposing the microconvection, generated by bubbles growing and departing in the immediate vicinity of the wall. Based on dimensionless groups derived by Stephan, an empirical correlation was developed by Kaufmann and Vaihinger [23]

$$Nu = \frac{\alpha D_{\text{bub}}}{\lambda_l} = 0.078 K_a^{0.62} \cdot K_b^{0.133} \cdot K_c^{0.634} \cdot K_d^{0.234} \cdot Pr^{1.032} \cdot Re^{0.078} \tag{3.44}$$

The dimensionless groups in Eq. (3.44) are formulated as follows

$$K_a = \frac{\dot{q} D_{\text{bub}}}{T_s c_l \eta_l}; \quad K_b = \frac{k}{D_{\text{bub}}}; \quad K_c = \frac{\varrho_l^2 (f D_{\text{bub}})^2 D_{\text{bub}}}{\sigma \rho_v}$$

$$K_d = \frac{\Delta h_v \varrho_l^2 D_{\text{bub}}^2}{\sigma^2 c_l T_s}; \quad Pr = \frac{\nu_l}{a_l}; \quad Re = \frac{(f D_{\text{bub}}) D_{\text{bub}} \varrho_l}{\eta_l}$$

and the bubble diameter can be calculated with Eq. (3.41). The product of the bubble departing frequency f and the bubble diameter was formulated by Kaufmann and Vaihinger in the equation

$$f D_{\text{bub}} = 0.314 \frac{g(\varrho_l - \varrho_v)}{\varrho_l}.$$

Completely different, however, is the situation if only a thin liquid film covers the wall which may be the case with cooling by falling film flow or by spraying liquid onto the surface. With this liquid layers at a hot surface which, however, is below the Leidenfrost-temperature, experiments showed that almost no bubbles are formed in this layer, and the evaporation takes place at the free surface of the liquid film. This evaporation mode is called "surface boiling", and the word surface stands here for the interface between the liquid and the ambient gaseous environment and not for the surface of the solid wall to be cooled. The heat is transported from the solid wall to the free surface, mainly by conduction and convection in the liquid film.

Up to now a fully theoretical description of this heat transport is not presented in the literature and therefore, the heat transfer coefficient with this evaporating mode is described by semi-empirical correlations. These semi-empirical correlations are based on the Martinelli-parameter X_{tt} which is formulated for turbulent conditions in the liquid film and in the gaseous environment:

$$X_{tt} = \left(\frac{\varrho_v}{\varrho_l}\right)^{0.5} \left(\frac{\eta_l}{\eta_v}\right)^{0.1} \left(\frac{1 - \dot{x}}{\dot{x}}\right)^{0.9} \tag{3.45}$$

and on the boiling number

$$Bo = \frac{q}{\dot{m}\Delta h_v}; \tag{3.46}$$

The equations given in the literature can be separated in two groups of the form

$$\frac{\alpha_{\text{surf. boil.}}}{\alpha_{\text{sing. phase}}} = A\left(\frac{1}{X_{tt}}\right)^b \tag{3.47}$$

or

$$\frac{\alpha_{\text{surf. boil.}}}{\alpha_{\text{sing. phase}}} = M\left[Bo \cdot 10^4 + N\left(\frac{1}{X_{tt}}\right)^n\right]^m. \tag{3.48}$$

Which form should be used depends on the fluiddynamic conditions in the film. If the film itself is purely of single-phase nature Eq. (3.47) can be used, however, if the liquid film is thicker and some bubble nucleation is to be expected, Eq. (3.48) should be preferred. If nothing is known about the single- or two-phase nature of the Film Eq. (3.48) should be preferred. The boiling number *Bo* in Eq. (3.48) takes into account some bubble formation in the liquid film which improves the heat transfer. Values for the constants A, M, N and the exponents b, n, m are given in Tables 3.1 and 3.2 for various substances and different flow directions.

In Eqs. (3.47) and (3.48) the heat transfer coefficient with evaporation is related to the heat transfer coefficient in purely single-phase forced or free convection. This heat transfer coefficient with free or forced single-phase convection can be calculated, using the equations given in Chap. 2.2. In the

Table 3.1. Values for A and b in Eq. (54)

	A	b
water, upflow	2.9	0.66
water, downflow	2.72	0.58
R113 upflow	4.0	0.37
n-butanol	7.5	0.328
org. liquids, nat. conv.	3.4	0.45

Table 3.2. Values for M, N, n and m in Eq. (55)

	M	N	n	m
water, upflow	0.739	1.5	2/3	1
water, downflow	1.48	1.5	2/3	1
R113 upflow	0.9	4.45	0.37	1
R12 horiz.	1.91	1.5	2/3	0.6
n-Butanol	2.45	1.5	2/3	1

Reynolds-number of these convective heat transfer correlations a superficial velocity has to be used which is calculated with the assumption that only liquid would be present in the channel. Using the Colburn-correlation, one can formulate this reference value of the single-phase heat transfer coefficient with the simple equation

$$\alpha_{\text{sing. phase}} = \frac{\lambda_l}{d_{\text{equ.}}} 0.023 \left[\frac{d_{\text{equ.}} \dot{m}(1-x)}{\eta_l}\right]^{0.8} \left[\frac{c_l \eta_l}{\lambda_l}\right]^{0.4}. \tag{3.49}$$

The Reynolds-number in this equation is formed with the dynamic viscosity of the liquid and by expressing the mass flowrate of the liquid only with the help of the quality $x = m_o/m$ were m is the total mass flowrate density of the liquid and the vapour.

We now need a criterion when to use this thin film or surface boiling correlations with falling film flow or spray-cooling. Under wetting conditions surface boiling always can be assumed if the thickness of the liquid film is smaller than the diameter of bubbles which would be formed with nucleate boiling. With forced convection two-phase flow, usually the Martinelli-parameter X_{tt}, is used as criterion for separating nucleate boiling and surface boiling. Figure 3.10 gives some help to estimate the border-value of X_{tt} between nucleate and surface boiling. From this figure we learn that for

$$\frac{1}{X_{tt}} > 5 \tag{3.50}$$

we always can assume surface boiling, and we can use Eq. (3.48) to calculate

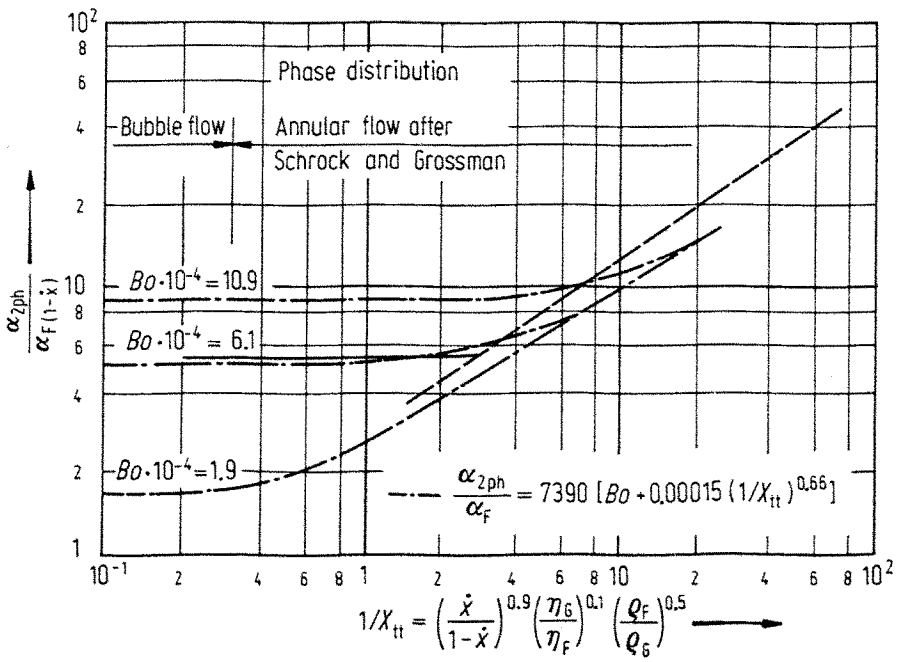

Fig. 3.10. Transition from nucleate boiling to surface boiling in annular flow

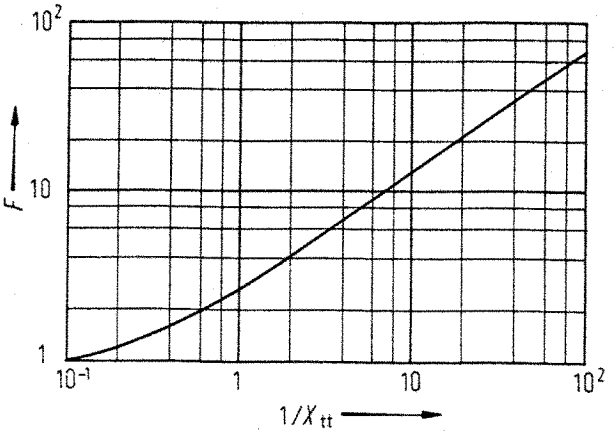

Fig. 3.11. Correction function F in Eq. (3.53) according to Chen [25]

the heat transfer coefficient. Below this value, one has to use pool boiling equations. Figure 3.10 shows also that this border-value of X_{tt} is a function of the boiling number.

For a rough estimation of the heat transfer coefficient with surface boiling in water, we can use Eq. (3.51)

$$\frac{\alpha_{\text{surf. boil.}}}{\alpha_{\text{sing. phase}}} = 0.065\left(\frac{1}{X_{tt}}\right)\left(\frac{T_s}{T_s - T_l}\right)\left(\frac{\sigma_{H_2O}}{\sigma_l}\right)^{0.9} \tag{3.51}$$

which was formulated by Calus [24] and which is much simpler to handle than Eq. (3.48).

In a different way as described above, the heat transfer with forced convection boiling is treated by Chen [25]. Similar as Rohsenow [22] he composes the heat transfer to the gas-liquid-mixture of two components, that of the boiling and that of the forced convection.

$$\alpha_{\text{boil}} = \alpha_{\text{sing. phase}} + \alpha_{\text{pool, boiling}}. \tag{3.52}$$

Unlike to Rohsenow he is not adding the heat flux densities, but the heat transfer coefficients. The reason for this is that he assumes that the driving temperature difference is the same for both mechanisms of heat transport. Chen recommends for calculating the convective contribution to the combined heat transfer coefficient the equation

$$\alpha_{\text{sing. phase}} = \frac{\lambda_l}{d_{\text{equ}}} 0.023\left[\frac{\dot{m}(1-x)d_{\text{equ}}}{\eta_l}\right]^{0.8}\left[\frac{\eta_l c_l}{\lambda_l}\right]F. \tag{3.53}$$

In this equation F is a correction factor which takes into account the different flow conditions in gas-liquid-mixtures compared to that in pure single-phase fluids. The temperature field is strongly influenced by the velocity gradient in the boundary layer near the wall, and this gradient again is depending on the sheer stress situation and the void fraction there. Both fluiddynamic situations can be expressed as a function of the Martinelli-parameter X_{tt}, assuming that both phases are in turbulent conditions. Therefore, it is reasonable to describe this correction factor F as a function of the Martinelli-parameter as shown in

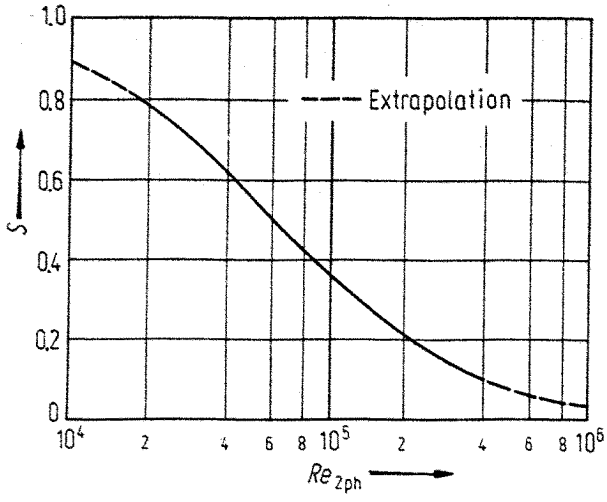

Fig. 3.12. Correction factor S in Eq. (3.54) according to Chen [25]

Fig. 3.11. According to Chen this course of the correction factor is valid over a wide range of void fraction or quality, reaching from nucleate boiling via surface boiling up to the onset of dry-out. With this correction factor and an equation for the heat transfer coefficient with nucleate boiling Chen succeeded in correlating the heat transfer in the whole range of vapour-liquid-mixtures, without splitting it in two regions as described before. The equation, recommended by Chen for the heat transfer coefficient with nucleate boiling is based on a correlation by Forster and Zuber [26]

$$\alpha_{\text{pool, boil}} = 0.00122\left[\frac{\lambda_l^{0.79} c_l^{0.45} \varrho_l^{0.49}}{\sigma^{0.5}\eta_l^{0.29}\Delta h_v^{0.24}\varrho_v^{0.24}}\right](T_{\text{Wall}} - T_s)^{0.24}\Delta p_s^{0.75} S \qquad (3.54)$$

and contains a correction factor S which takes into account the temperature situation in the boundary layer. This correction S depends on the two-phase Reynolds-number

$$Re_{2ph} = \left[\frac{\dot{m}(1-x)}{\eta_l d_{equ}}\right] F^{1.25}, \qquad (3.55)$$

as shown in Fig. 3.12. So Chen combines the mechanism of nucleate boiling with that of forced convection and the correction factor F stands for the sheer stress induced velocity field. The temperature difference $\Delta T_s = T_{\text{Wall}} - T_s$ is the superheating of the liquid in the immediate vicinity of the wall and by this is a measure of the driving force for nucleation and bubble growth.

Equation (3.54) is an empirical correlation and was presented by Chen in a non-dimensionless form. Therefore, one has to choose the right dimensions when using it, namely the international system with the mass in kg, the length in m, the force in N and the energy in J. The pressure must be given in N/m^2. The calculation procedure is a little complicated because, depending on the boundary conditions an iterative method has to be used. It is recommended to start with calculating the heat transfer coefficient for forced convection single-phase flow and with evaluating the correction factor F. For boundary

conditions with given heat flux then the wall temperature has to be estimated, and the estimation has to be improved in a proper way during the iteration.

3.3.3 Heat Transfer with Film Boiling

Heat transfer with film boiling is of complete different nature compared to that of nucleate boiling. With film boiling the wall is unwetted due to its high temperature and the heat transport has been managed through a thin vapour film from the wall to the saturated liquid. Film boiling occurs at high heat fluxes beyond the so-called critical heat flux and as shown in Fig. 3.13 bubbles separate from the vapour film adjacent to the wall and travel into the saturated liquid. The heat transfer process can be easily described, if one assumes that the vapour in the film flows in a laminar configuration and if one neglects the small sheer stress between the phase interface of vapour and liquid. In addition one can assume that the distance between two bubble columns separating from the film can be expressed by the Taylor- or Helmholtz-instability depending on whether the film is horizontally or vertically orientated. One then ends up with the well-known equations by Bromley [27] or Berenson [28]. These heat transfer correlations are similarly derived as the equations for film condensation which are based on the falling liquid film theory by Nusselt. For a detailed information concerning these theoretical models reference is made to papers by Hsu [29] and Bressler [30].

Assuming turbulent flow in the vapour film, one can also start from the laws for mixed convection for vertically orientated vapour films and one then ends up with a correlation for describing the heat transfer coefficient, which contains a Reynolds-number referred to the thickness of the liquid film, a modified Grashof-number and the Prandtl-number. There are also correlations based on the turbulent boundary layer theory which take in account the effect of interface oscillations between the phases. These oscillations improve the heat transfer.

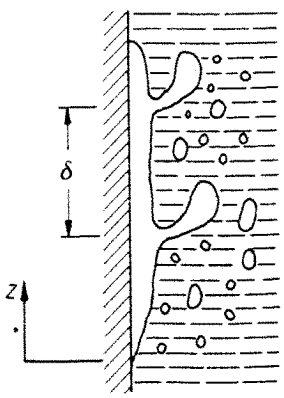

Fig. 3.13. Situation with film boiling at the Ball

Based on the equation by Bromley

$$\alpha_{\text{film, boil}} = 0.62\left[\frac{\lambda_v^3 \varrho_v(\varrho_l - \varrho_v)\Delta h_v g}{\eta_v(T_v - T_s)\delta_{\text{hor}}}\right]^{0.25} \tag{3.56}$$

Hsu [31] developed the equation

$$\alpha_{\text{film, boil, hor.}} = 1.456\cdot 10^3 \cdot \exp(-3.76\cdot 10^{-3}\cdot p^{0.1733})\{T_v - T_s\} + 0.62\left[\frac{\lambda_v^3 \varrho_v(\varrho_l - \varrho_v) g \Delta h_v}{\eta_v(T_v - T_s)\delta_{\text{hor}}}\right]^{0.25}. \tag{3.57}$$

This equation is valid for a horizontal orientation of the vapour film and contains the distance δ_{hor} between the vapour columns separating from the film which can be calculated from Eq. (3.58)

$$\delta_{\text{hor}} = 2\pi\left[\frac{\sigma}{g(\varrho_l - \varrho_v)}\right]^{0.5} \tag{3.58}$$

based on the theory for Taylor-instabilities. The second term of Eq. (3.57) represents a pressure correction. For vertical orientation Leonhard [32] uses the Helmholtz-instability for the distance of the separating bubbles representing a characteristic length δ_{vert}

$$\delta_{\text{vert}} = 16.24\left[\frac{\sigma^4 \Delta h_v^3 \eta_v^5}{\varrho_v(\varrho_l - \varrho_v)^5 g^5 \lambda_v^3 (T_{\text{wall}} - T_s)^2}\right]^{0.5} \tag{3.59}$$

which he then implements in Bromley's-equation Eq. (3.56). Sherman and Sabersky [33] made an interesting proposal for correlating heat transfer with film boiling at vertically orientated surfaces. They introduce a dimensionless heat transfer coefficient N_α

$$N_\alpha = \frac{\alpha}{\varrho_v c_v\left(\frac{\eta_v g}{\varrho_v}\right)^{1/3}} \tag{3.60}$$

which they describe as a function of the physical properties of the vapour in the film.

$$N_\alpha = 0.22\left(\frac{\varrho_l}{\varrho_v}\right)^{1/3} Pr_v^{-0.65}\left(\frac{c_v(T_{\text{wall}} - T_s)}{\Delta h_v}\right)^{-0.23}. \tag{3.61}$$

Compared with the literature describing nucleate boiling, papers on film boiling are much more rare, and measured values show larger tolerances. The reason for this is the high temperature under which the measurements have to be performed and also the difficulties of the measuring techniques under these high temperatures. The situation with respect to reliable data becomes even worse if one looks for heat transfer measurements in subcooled film boiling. With subcooled liquid. The fluiddynamic phenomena at the phase interface change remarkably because the condensation of the vapour at the subcooled liquid

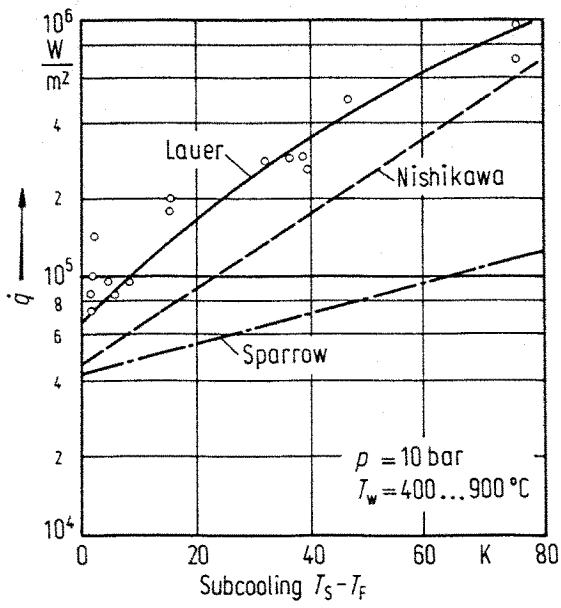

Fig. 3.14. Heat flux with film boiling in subcooled water at 10 bar

surface produces high acceleration forces towards the interface and also towards the wall which can induce local rewetting for a short period. Also the turbulence in the vapour film is strongly increased. Lauer [8], Nishikawa [34] and Sparrow [35] showed within a certain agreement and as demonstrated in Fig. 3.14 that with film boiling in subcooled liquids much higher heat fluxes can be transferred than in saturated liquids.

3.3.4 Transition Boiling

As we saw in Fig. 3.1 when we discussed the Nukijama-curve, there is a region between critical heat flux and fully developed film boiling which is called transition boiling. In this region a heat transfer mechanism can be observed which gives decreasing heat transfer coefficients with increasing temperature difference between wall and fluid. Visual observations of the fluiddynamic situation give the impression as if the hot wall would be temporally wetted so that periods of nucleate boiling change with that of film boiling.

A detailed literature survey on heat transfer under the conditions of transition boiling is given by Groeneveld and Fung [36]. These authors defined the transition boiling as a combination of unstable film boiling and unstable nucleate boiling. The later one plays the more important role for the heat transfer process from the wall to the fluid. This means that correlations used for nucleate boiling could be also of some relevance for describing transition boiling.

Starting from the idea that the heat transfer with transition boiling is strongly depending on the short-time rewetting of the wall and by this on bubble boiling, in the literature frequently correlations can be found of the form

$$q = Ae^{-B(\Delta T)} \tag{3.62}$$

This form implements the difficulty to describe the coefficients A and B in a physically proper way. A simple method is to formulate A and B as a function of the physical properties of the fluid. However, also the temperature difference ΔT between the rewetting temperature—the Leidenfrost-temperature—and the saturation temperature plays a role. As an example of these kinds of equations here the correlation by Tong [9] is presented

$$\dot{q} = \dot{q}_{\text{sing. phase}} \cdot \exp\left[-0.001 \frac{X_{\text{equ}}}{\frac{dx_{\text{equ}}}{dz}} (\Delta T/100) \right]^{1+0.0016\,\Delta T} \tag{3.63}$$

This equation was originally developed to describe the cooling phenomena in nuclear reactors under the conditions of a loss of coolant accident. Applying Eq. (3.63) one has to know the heat flux $q_{\text{sing. phase}}$ which would exist with purely single phase liquid flow, i.e. without boiling. This heat flux can be calculated by using the equations given in the previous chapters. In addition the change of the quality $x_{\text{equ.}}$ with respect to the coordinate in flow direction must be known. This can be calculated by assuming thermal equilibrium.

Another form of correlating heat transfer coefficients with transition boiling was presented by Dhir [37]. Dhir evaluated his equation from his measurements where he immersed cooper- and silver-spheres into water which was subcooled up to 60 K. Dhir used the Jakob-number as describing parameter.

3.3.5 Critical Heat Flux

For applying heat transfer correlations under high heat flux densities one has to know the boiling mode—nucleate, transition or film boiling. There exist numerous correlations in the literature predicting the critical or peak heat flux with pool boiling. Several examples for these correlations could be cited, however, here only the form elaborated by Zuber [38] shall be presented

$$\dot{q}_{\text{crit}} = 0.131 \Delta h_{\text{v}} \varrho_{\text{v}} \left[\frac{\sigma(\varrho_{\text{l}} - \varrho_{\text{v}})g}{\varrho_{\text{v}}^2} \right]^{1/4} \tag{3.64}$$

The constant in Eq. (3.64) as originally proposed by Zuber was 0.131, however, this value is generally considered to be low and Rohsenow [39] proposed the value 0.18.

While this correlation describes quite well sets of data measured in water it is not accurate for all systems. For example, the predicted critical heat fluxes are widely divergent for boiling liquid oxygen.

Considerable progress has been made in accounting for the effects of heater geometry. Sun and Lienhard [40], Lienhard and Dhir [41] and Lienhard and Riherd [42], re-examined the model by Zuber and found that the vapour-removal configuration varies according to the heater geometry and size. A simple

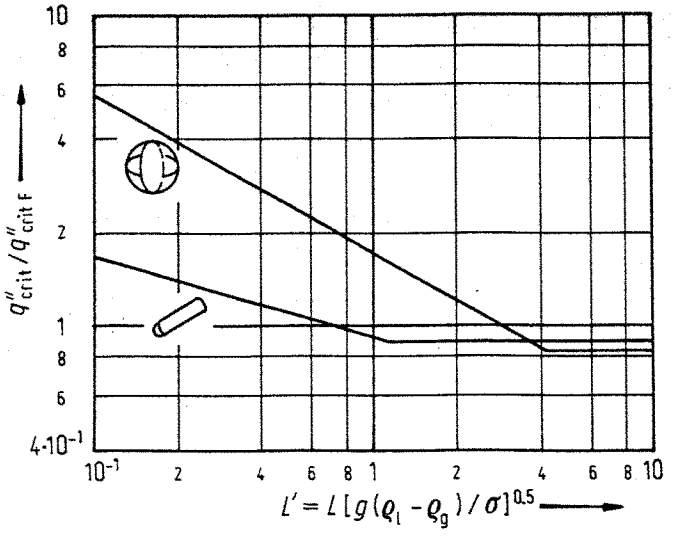

Fig. 3.15. Critical heat flux in water with various heater configurations according to Bergles [48]

correction can be made by using a characteristic length L'

$$L' = L[g(\varrho_l - \varrho_v)/\sigma]^{1/2}. \tag{3.65}$$

The correlation for this characteristic length then serves as a correction factor for the critical heat flux taking into account the heater geometry and its size

$$\dot{q}''_{crit}/\dot{q}''_{crit,F} = f(L'). \tag{3.66}$$

Results of semi-empirical correlations are summarized in Fig. 3.15. They indicate that the correlation curves vary according to geometry for small heaters and are also generally different for large heaters. These correlation curves were based on a large number of data points.

Although the experimental verification is difficult, data for large flat plates (facing up) tend to substantiate the semi-empirical prediction for an infinite flat plate

$$\dot{q}''_{crit}/\dot{q}''_{crit,F} = 1.14. \tag{3.67}$$

Nucleate boiling and the associated hydrodynamic instabilities vanish for very small heaters ($L' < 0.01$ mm) and therefore with increasing heat flux natural convection proceeds directly into film boiling.

For forced convection boiling the prediction of the critical heat flux is much more complicated and strongly depending on the heater geometry as well as on the fluiddynamic conditions. For finding correlations to predict critical heat flux under these conditions reference is made to the book by Collier [43].

3.3.6 Immersion Cooling

With immersion cooling, as it is usual in the quench hardening treatment, several thermo- and fluiddynamic modes—starting from film boiling via transition

boiling and nucleate boiling up to single-phase free convection—can exist. The heat transfer process is primarily depending on the surface temperature of the immersed body, however, also on its thermal conductivity near the surface and its surface roughness.

With hardening usually the temperature of the body is known before dipping it into the quenching bath and in most cases this temperature is above the Leidenforst-temperature. So film boiling will start immediately after dipping.

The lower limit of stable film boiling corresponds to the onset of liquid-solid contact. Numerous analyses have been made to predict this condition, generally based on hydrodynamic stability theory similar to that employed in determining the critical heat flux. For a flat horizontal surface the minimum heat flux can be calculated by an equation given by Zuber [44]

$$q_{\min} = C\Delta h_v \varrho_v \left[\frac{\sigma g(\varrho_l - \varrho_v)}{(\varrho_l + \varrho_v)^2}\right]^{1/4} \tag{3.68}$$

where C is variably given as 0.177 [46] or 0.09 [47].

For small bodies—wires—it is necessary to account for curvature effects and especially for the effect of surface tension in the transverse direction upon the Taylor- instability of the interface. Lienhard and Wong [48] have suggested the following semi-empirical equation

$$q_{\min} = 0.057 \frac{\varrho_v \Delta h_v}{R}\left[\frac{2g(\varrho_l - \varrho_v)}{(\varrho_l + \varrho_v)} + \frac{\sigma}{(\varrho_l + \varrho_v)^2}\right]^{1/2} \cdot \left[\frac{g(\varrho_l + \varrho_v)}{\sigma} + \frac{1}{2R^2}\right]^{-3/4}. \tag{3.69}$$

This equation should be used for curvatures of small radii (below 2 nm) only. For larger curvatures Eq. (3.68) may be applied. However, Kovalev [49] notes that this equation overpredicts the data for water on clean surfaces at pressures above atmospheric pressure.

In any case these equations cannot be relied upon for systems where the liquid contains impurities and the surface exhibits some degree of contamination. Oxidation increases wettability.

Also from another point of view it is difficult to calculate the minimum heat flux of film boiling. The energy balance demands that the heat flux transported by conduction in the solid material to its surface must be the same as the heat flux transported by film boiling or nucleate boiling from the surface to the fluid. So the moment when film boiling ends has always to be determined in an iterative way by using Eq. (3.68) and by calculating the conductive heat flux to the surface.

The period of transition boiling—after the minimum heat flux was reached—is usually very short and can be neglected for most practical cases. Therefore, one can assume that when the vapour film has collapsed, nucleate boiling starts. For the following period the heat transfer coefficient can be calculated with the correlations given in the chapter on nucleate boiling. Here again, we have to

observe the balance between heat conducted to the wall and heat transported from it by nucleate boiling. When the surface temperature of the wall reaches the saturation temperature nucleation stops and the heat transfer is furtheron managed by liquid free convection only. For calculating this period reference is made to the chapter on free convective heat transfer.

List of Symbols

A	area
A	constant
a	pitch-diameter-ratio perpendicular to flow
a	thermal diffusivity
b	pitch-diameter-ratio longitudinal to flow
Bo	boiling number
c	specific heat capacity
c_F	specific heat capacity of the liquid
C_F	factor representing properties of liquid
C_w	factor representing properties of a heated wall
D	diameter
CHF	critical heat flux
DNB	departure from nucleate boiling
f	bubble departing frequency
F	correction factor
Gr	Grashof number
g	standard acceleration due to gravity
h_l	enthalpy of liquid
h_v	enthalpy of vapour
k	roughness depth
L	characteristic length
M	constant
$\dot{M}$	mass flow
$\dot{m}$	mass flow rate density
N	constant
Nu	Nusselt number
N_α	dimensionless heat transfer coefficient
p_l	pressure of liquid
p_v	pressure of vapour
Pe	Peclet number
Pr	Prandtl number
$\dot{q}$	heat flux density
$\dot{Q}$	heat flow rate
R	bubble Radius
Re	Reynold number

S	correction factor
T	temperature
T_s	saturation temperature
T_v	vapour temperature
$T_v - T_s$	superheating temperature
v_l	specific volume of liquid
v_v	specific volume of vapour
w	velocity
$\dot{x}$	specific vapour flow rate or vapour quality
X	Martinelli parameter
α	heat transfer coefficient
β	contact angle of bubble
β	volume coefficient of expansion
δ_{hor}	distance in horizontal direction
δ_T	thickness of thermal boundary-layer
δ_W	boundary-layer-thickness of velocity field
η	dynamic viscosity
λ	heat conductivity
ν	kinematic viscosity
Φ	two phase flow multiplier
ψ	friction factor
ϱ_l	density of liquid
ϱ_v	density of vapour
σ	surface tension
τ	shear stress
ϑ	temperature

List of Subscripts

bulk	condition in the core
boil	boiling
bub	bubble
conv.	convective
crit	critical
equ	equivalent
hor	horizontal
l	liquid
max	maximum
min	minimum
s	surface
sing.phase	single phase
surf.boil	surface boiling
v	vapour

x	x-direction
y	y-direction
z	z-direction

References

1. Jakob M (1936) In: Mech. Engng. 58: 643–660, 729–739
2. Fritz W (1935) In: Physik. Z. 36: 379–384
3. Jakob W, Linke (1935) In: Physik. Z. 36: 267–280
4. Bosnjakovic F (1930) In: Techn. Mech. Thermo-Dynam. 1: 358–362
5. Nukiyama VJ (1934) In: Jap. Mech. Engr. 37: 53–54, 367–374
6. Yao SC, Henry RE (1978) Experiments of quenching under pressure. Proc. 6th Intern. Heat Transfer Conf., Toronto, Canada
7. Hein D (1980) Modellvorstellungen zum Wiederbenetzen durch Fluten. Diss., Univ. Hannover, Inst. f. Verfahrenstechn.
8. Lauer H (1976) Untersuchung des Wärmeübergangs und der Wiederbenetzung beim Abkühlen heißer Metallkörper. Diss., Univ. Hannover, Inst. f. Verfahrenstechn.
9. Tong LS, Young JD (1974) A phenomenological transition and film boiling heat transfer correlation. Proc. 5th Intern. Heat Transfer Conf., Tokio
10. Forster HK, Zuber N (1954) In: J. Appl. Phys. 25: 474–478
11. Han CY, Griffith P (1965) In: Int. J. Heat and Mass Transfer 8: 887–904, 905–914
12. Plesset MS, Zwick SA (1954) In: J. Appl. Phys. 25: 493–500
13. Beer H (1969) In: Progr. Heat Mass Transfer 2: 311–370
14. Winter ERF, Matekunas FA (1971) An Inteferometric study of nucleate boiling. Int. Symp. on Two-Phase Systems, 29, Aug. – 2, Sept. Haifa, Israel
15. Mayinger F, Panknin W (1974) Holography in heat and mass transfer, Vol. 6, p. 28–43 Proc. 5th Int. Heat Transfer Conf., Tokio
16. Grigull U (1961) Wärmeübertragung, Springer-Verlag, Berlin
17. Schlünder EU (1983) Einführung in die Wärmeübertragung, 4. Aufl., S. 103. Vieweg (Verlag), Braunschweig
18. Hausen H (1959) Neue Gleichungen für die Wärmeübertragung bei freier oder erzwungener Konvektion. In: Allgem. Wärmetechnik 9: 75–79
19. Hausen H (1969) Bemerkung zur Veröffentlichung von A. Hackl und W. Gröll, Zum Wärmeübergangsverhalten zähflüssiger Öle. In: Verfahrenstechn. 3: 355, 480 (Berichtigung)
20. Choi H, Rohsenow WM (1961) Heat, mass und momentum transfer. Englewood Cliffs, Prentice Hall
21. Stephan K, Preußer P (1979) Wärmeübergang und maximale Wärmestromdichte beim Behältersieden binärer und ternärer Flüssigkeitsgemische. In: Chem.-Ing.-Techn. MS 649/79, Synopse Chem.-Ing.-Techn. 51: 37
22. Rohsenow WM (1963) Modern Developments in Heat Transfer, p. 85–158. Academic Press, New York
23. Vaihinger D, Kaufmann WD (1972) In: Chem.-Ing.-Techn.: 921–927
24. Calus WF et al. (1972) In: Chem. Engng. J. 6: 223–250
25. Chen JC (1966) Correlation for boiling heat transfer to saturated liquids in convective flow. Int. Eng. Chem. Process Design and Development 5, p. 322
26. Forster HK, Zuber N (1955) Dynamics of vapour bubbles and boiling heat transfer. In: AIChE Journ. 1(4): 531–535
27. Bromley LA (1950) In: Heat transfer in stable film boiling. Chem. Eng. Progr. 46: 221–227
28. Berenson PI (1962) Experiments on pool boiling heat transfer. In: Int. J. of Heat and Mass Transfer 5: 985–999
29. Hsu YY (1972) In: Adv. Cryogenic Engng. 17, p. 361
30. Bressler RG (1972) Adv. Cryogenic Engng. 17, p. 382
31. Hsu YY (1975) Tentative correlations of reflood heat transfer. LOCA-research Highlights, (Apr. 1 – June 30)

32. Leonhard JE, Sun KH, Dix GE (1977) Solar and nuclear heat transfer. In: AIChE Symp. 73, No. 164: 7
33. Shermann DC, Sabersky RH. Natural convection film boiling on a vertical surface. Persönliche Mitteilung
34. Nishikawa KT, Ito T (1966) In: Int. J. Heat and Mass Transfer 9: 103
35. Sparrow EM, Cess RD (1962) In: J. Heat Transfer 84: 55
36. Groeneveld DC, Fung KK (1976) Forced convective transition boiling. Review of literature and comparison of prediction methods. In: AECL-Report p. 5543
37. Dhir VK (1978) Study of transient transition boiling heat fluxes from spheres subjected to forced vertical flow. Proc. 6th Int. Heat Transfer Conf., Toronto, Canada
38. Zuber N, Tribus M, Westwater JW (1961) The hydrodynamic crisis in pool boiling of saturated and subcooled liquids. Int. Develop. in Heat Transfer, Part II, ASME, p. 230–235
39. Rohsenow WM and Griffith P (1956) Correlation of maximum heat transfer data for boiling of saturated liquids. In: Chem. Eng. Progr., Symp. Series 52, No 18: 47–49
40. Sun KH, Lienhard IH (1970) The peak pool boiling heat flux on horizontal cylinders. In: Int. J. of Heat and Mass Transfer 13: 1425–1439
41. Lienhard IH, Dhir VK (1973) Hydrodynamic prediction of peak pool boiling heat fluxes from finite bodies. In: J. Heat Transfer 95: 152–158
42. Lienhard IH, Dhir VK, Riherd DM (1973) Peak boiling heat flux measurements on finite horizontal flat plates. In: J. Heat Transfer 95: 477–482
43. Collier JG (1981) Convective Boiling and Condensation, 2nd edn. McGraw Hill, New York
44. Zuber N (1958) On stability of boiling heat transfer. In: Trans ASME 80: 711–720
45. Berenson PJ (1961) Transition boiling heat transfer from an horizontal surface. In: J. Heat Transfer 83: 351–358
46. Lienhard IH, Wong PTY (1964) The dominant instable wavelength and minimum heat flux during film boiling on an horizontal cylinder. In: J. Heat transfer 86: 220–226
47. Kovalev SA (1966) An investigation of minimum heat fluxes in pool boiling of water. In: Int. J. of Heat and Mass Transfer 9: 1219–1226
48. Bergles AE (1975) Burnout in Boiling Heat Transfer, Part I Pool Boiling Systems. In: Nuclear Safety 16: 29–42